THESIS FOR THE DEGREE OF LICENTIATE OF ENGINEERING IN THERMO AND FLUID DYNAMICS

MULTICOMPONENT SPRAY-TURBULENCE INTERACTION

VIGNESH PANDIAN MUTHURAMALINGAM

Department of Mechanics and Maritime Sciences
CHALMERS UNIVERSITY OF TECHNOLOGY

Gothenburg, Sweden 2018

MULTICOMPONENT SPRAY-TURBULENCE INTERACTION
VIGNESH PANDIAN MUTHURAMALINGAM

Thesis for the degree of Licentiate of Engineering 2018:08
Department of Mechanics and Maritime Sciences
Chalmers University of Technology
SE-412 96 Gothenburg
Sweden
Telephone: +46 (0)31-772 8221

Chalmers Reproservice
Gothenburg, Sweden 2018

MULTICOMPONENT SPRAY-TURBULENCE INTERACTION
Thesis for the degree of Licentiate of Engineering in Thermo and Fluid Dynamics
VIGNESH PANDIAN MUTHURAMALINGAM
Department of Mechanics and Maritime Sciences
Chalmers University of Technology

Abstract

Blended fuels are gaining importance in automotive industry owing to stringent legislations for emissions. It is important to understand the fuel spray formed as a consequence of injecting blended fuels into the engine (for direct injection engines) and also the influence of fuel spray on combustion properties. Fuel sprays are sought to be understood by formulating and modelling the physical processes involved in its formation and testing the predictions obtained from models using computer simulations. Complementing this procedure, experiments are performed under predefined boundary conditions either in single or multi cylinder engines or in constant volume spray chambers when deeper insight into sprays is required. The experiments are used to validate the models and also report any newly observed physical phenomenon which can be then investigated using the models.

This work presents the computaional and modelling efforts for multicomponent fuel sprays whose behavior is studied in constant volume combustion vessel. Lagrangian-Eulerian framework is followed where the liquid fuel is modelled using Lagrangian approach and the gas phase is modelled using Eulerian approach. The focus of this work is on Lagrangian liquid phase modelling and it's interactions with the gas phase. The spray modelling is done using VSB2 stochastic blob and bubble (VSB2) model which is developed with the aim of minimising tuning parameters by treating spray and it's submodels as one entity. The VSB2 model also removes overshoot or undershoot in predicted quantities by using relaxation equations based on thermodynamic equilibrium. The methods for modelling secondary breakup, evaporation and momentum transfer of liquid droplets are outlined in this work. Specifically computational method for differential evaporation in multicomponent fuel sprays is discussed.

The VSB2 model is validated against experiments performed in constant volume combustion vessels for multicomponent fuel sprays. Differential evaporation was predicted corrrectly by the model within acceptable limits when compared to experiments on component gasoline-diesel fuel blend. Effects of non-ideal vapor liquid equilibrium on multicomponent fuel evaporation of ethanol and iso-octane blend was also studied, and the predictions showed reasonable agreement with experiment. Ethanol was observed to have a strong influence on iso-octane and deviation from ideal behavior was strong for higher ethanol percentage and in these cases ideal vapor liquid equilibrium was seen to predict incorrect results.

Keywords: Stochastic Blob and Bubble (VSB2) spray model, CFD, multicomponent fuel sprays, direct injection engines, gasoline/diesel blend, ethanol/iso-octane blend

List of publications

This thesis is based on the work contained in the following publications:

Publication A Muthuramalingam, Vignesh Pandian and Karlsson, Anders, "Development and Validation of a Multicomponent Fuel Spray Model (VSB2 Model)" in *SAE 2017- International powertrains fuels and lubricants meeting, Beijing, China* .

Publication B Muthuramalingam, Vignesh Pandian and Karlsson, Anders, "Influence of considering non-ideal thermodynamics on droplet evaporation and spray formation (for gasoline direct injection engine conditions) using VSB2 spray model" in *WCX^{TM} 18: SAE world congress experience, Detroit, MI, US* .

Acknowledgements

It's been a great time learning, working and having fun in the division and in the time period altogether that I have spent working so far. For this I have to acknowledge a lot of people. First I would like to thank my main supervisor Anders Karlsson, and CERC director Ingemar Denbratt for giving me the opportunity to work in this project. I thank Anders Karlsson for the patient long discussions while writing down equations on white board and explaining VSB2 and also all the support throughout the project. I also thank my co-supervisor Michael Oevermann for his guidance in the project.

Apart from this I want to acknowledge my office mates, Michael and Andreas for the daily chit chats. I cannot forget all my fellow PhD students in the division who were there during good and tough times for chats during fikas, lunches and afterworks and played an important role during the period I worked so far. I want to acknowledge the good times and conversations I had with research engineers and teaching/research staff who also contributed to make a good working environment for me. Indeed I thank Elenor for organizing lovely christmas dinners and summer lunches.

Last but not the least I cannot conclude without acknowledging my parents and my brother for their endless support.

Contents

1 Introduction

The change in global oil demand sectorwise as projected by International energy agency for the future, indicates that although there will be a reduction in demand by passenger vehicles, there will still be a large demand from aviation, shipping and road freight sectors (trucks)[1]. Even if there is reduction in demand, passenger vehicles are still projected to consume fossil fuels. It is important therefore to complement if not replace the consumption of fossil fuels with alternate energy sources such as renewable fuels. For this reason, there has been increased focus on blended fuels, where conventional fuels are blended with biofuels. Apart from the problem of depleting fossil reserves, combustion of fossils creates by products that are proven to be harmful for environment and human health. It is therefore important to minimize the emission of harmful byproducts of combustion.

With respect to transport sector, in order to use new fuels (such as blended fuels) in existing engines, it is important to understand the spray formation and combustion charecteristics as they will be different when using different fuels. The combustion process, in specific for a compression ignition type of engine, can be conceptually divided into two parts: fuel spray formation and combustion. The fuel spray formation consists of the following sequence of events: injection of fuel followed by atomization and breakup, droplet collision/coalescence, droplet eavporation and mixture formation. The fuel mixture than ignites and chemically reacts, leading to combustion. In order to predict combustion properties such as emission and fuel consumption, it is therefore imperative to understand evaporating and combusting fuel sprays.

Fuel sprays and combustion charecteristics are analyzed by performing experiments in engines, or closed/open, constant volume spray chambers. To complement this method, computaional fluid dynamics (CFD) simulations are performed under similar boundary conditions having the benefit of decreased setup cost and depending on the case, even reduced time. While CFD simualations have the advantage of low cost of equipments, it relies on experimental input for accuracy and validity of predictions and hence both the methods go hand in hand. This work focuses on CFD simulations of fuel sprays, and in specific multicomponent fuel spray modelling.

1.1 Fuel spray modeling

A schematic of fuel spray obtained from simulations(in this case injection of n-dodecane in constant volume combustion vessel) is shown in figure 1.1.
Fuel is injected at high pressure (around 200MPa for currently used heavy duty engines) from an injector which comprises of needle, sac and injection hole. Modern day engines have injection holes smaller than $100\mu m$ for light duty and smaller than $200\mu m$ for heavy duty engines. The core of the fuel spray consists of dense liquid which enters the combustion chamber with velocities around 600m/s. The liquid core entering combustion

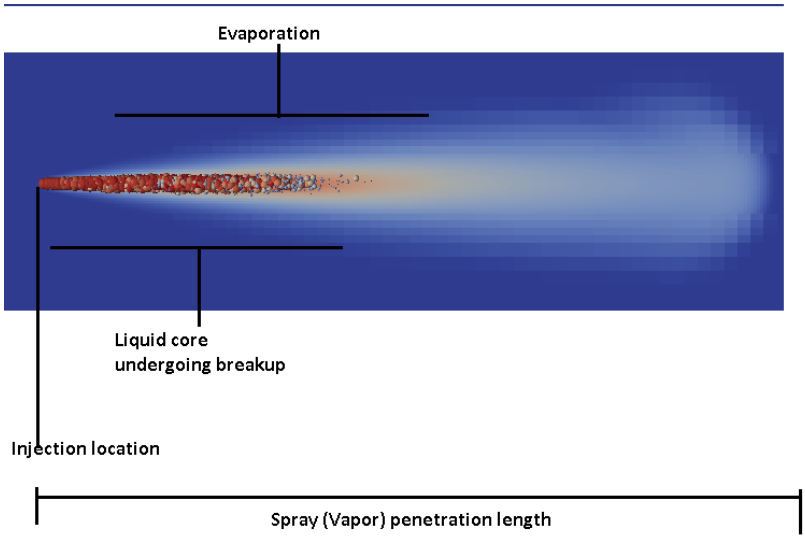

Figure 1.1: *Conceptual evaporating fuel spray*

chamber undergoes primary breakup to disintegrate into large ligaments and droplets which give the core a dense shape. Following primary breakup the larger droplets break into still smaller ones owing to aerodynamic forces, and this process is summed up as secondary breakup. The smaller droplets evaporate in to the surrounding air owing to heat transfer from hot air to the colder droplets. Eventually a conical spray is formed which is diluted further away from the nozzle due to air entrainment. The evaporation of spray, depends on the pressure and temperature of ambient gas. At high temperatures and pressures evaporation can take place at supercritical conditions. The length of liquid core from injector is commonly referred to as liquid length and the length of furthest tip of spray (usually guaged in terms of fuel vapor mass fraction) from injector is referred to as spray or vapor penetration. The fuel spray mixes with air, and eventually ignites due to chemical reactions providing the fuel with activation energy in order to combust. The high pressure from expanding gases following combustion, produces work on the piston. Fuel spray modelling comprises of computaional models describing all the processes starting from injection of fuel till the formation of combusting fuel spray. This work focusses on fuel spray modelling for non-combusting fuel spray, specifically on secondary breakup and evaporation.

1.1.1 Mutlicomponent fuel spray modelling

Automotive industry is focussing on increasing the use of blended fuels where conventional fuels are blended with biofuels, in an effort to comply with EU's aim of having 10% of transport fuels coming from renewable sources such as biofuels by 2020 [2]. With respect to the design of combustion process in an engine, it is a challenge to understand the influence of multicomponent fuels on spray formation and combustion.

Multicomponent fuel spray models fall into two broad categories namely discrete and continuous respectively (refer [3] under Evaporation of Multi-Component Droplets). In continuous multicomponent fuel spray model, a distribution function is used to estimate the mole fraction of each component in liquid and vapor phase based on molecular weight. It is based on continuous thermodynamics. In discrete model on the other hand, each component is treated as discrete entity and tracked individually during evaporation process. The advantage of discrete model is that it allows for coupling with reaction kinetics of each component. However, it is computationally expensive when compared to continuous model. Ra and Reitz [4] have developed and validated a discrete multicomponent fuel model where, the fuel components are treated as discrete species. Yang et.al [5] developed a hybrid discrete and continuous multicomponent model in which gasoline was assumed to consist of five different families of hydrocarbons. Each family is composed of an infinite number of continuous compounds, modelled as a probability density function (PDF), and the mass fraction of each family of hydrocarbon is in turn represented by another PDF, and the mean and variance of each pdf are tracked. Both Ra and Yang modelled realistic fuels (in case of Ra [4] gasoline and diesel, and in case of Yang [5] gasoline fuel) and produced confirming results with experiments.

1.1.2 Challenges in fuel spray modelling and issues addressed in this work

Some of the important challenges in fuel spray modelling are grid and time step dependencies and dependence of spray simulations on tuning parameters. Fuel sprays are examples of two phase flows consisting of liquid droplets penetrating into ambient gas. The most common way to simulate fuel sprays is Eulerian-Lagrangian approach. The gas phase is solved using the Eulerian approach and the liquid phase by Lagrangian approach. It is important to resolve the Eulerian phase spatially, and obtain the correct gas phase quantities to calculate ineraction with the Lagrangian phase. The Eulerian lagrangian method however imposes the constraint that void fraction should be close to unity, which implies that the volume of liquid should be small compared to that of gas in a grid cell. Due to this constraint it is not possible to continue reducing grid size until all the gas phase quantities are resolved. The conclusion from Engine combustion network (ECN) 1 workshop [6] is that using grid sizes smaller than 0.125mm for spray simulations of injectors with nozzle diameter 0.09mm, would result in violation of Eulerian-Lagrangian assumption. However, close to the nozzle it is important to have fine grid cells because the intial velocity gradients between liquid and gas phase are important to be resolved accurately. In the case of a gas jet impinging in gaseous atmposphere (Eulerian-Eulerian approach), Abraham [7] suggested that near the nozzle, jet cross sectional area should be resolved by at least 4 cells. As far as the time step dependency for spray simulations is considered, the vapor penetration is less dependent [6]. The liquid penetration however, is dependent on timestep [6] and a sensitivity analysis is often performed for the case under study to determine optimal time step.

Dependence of spray models on tuning parameters is another challenge. All the submodels in the spray model for instance- breakup, evaporation, heat transfer could

require their own tuning parameters which increase the total parameters. It is therefore a challenge to minimise the tuning parameters and also minimise tuning itself for different operating conditions.

The above mentioned challenges are addressed in this work. Apart from that certain issues in implementation of spray models are also addressed. The implementation of differential evaporation for multicomponent fuels is one of the issues. This is because complexity of implementation tends to increase with the number of fuel components. The question of method of treating vapor liquid equilibrium for evaporation of multicomponent fuels is another issue that has been discussed in literature. Ideal vapor liquid equilibrium neglects intermolecular interactions. While this approach may be suitable for single component fuels, it comes into question when considering multicomponent fuels. Certain pairs of molecules are known to have stronger interaction than others.

The rest of chapters in this text are ordered as follows; chapter 2 gives an overview of basic gas phase equations and a description of VSB2 model with focus on multicomponent fuel evaporation and non-ideal vapor liquid equilibrium; chapter 3 gives an overview of the experimental, computational setup and also brief information on the submodels used for simulations; chapter 4 summarises two recent publications on spray simulations using VSB2 model which are validated with experimental data and chapter 5 provides an overview of future plans for model development.

2 Methodolgy and modelling approach

This chapter summarises the decription of spray model. Spray formation involves interaction between the liquid and gas phases. The gas phase is solved using Eulerian approach and the liquid phase is solved using Lagrangian approach. Both these approaches and also their interactions are described in the following sections.

2.1 Eulerian phase

The gas phase is solved using the Eulerian approach in which transport equations are solved for mass, energy and momentum of gas. The continuity equation is given by Eq 2.1

$$\frac{\partial \rho}{\partial t} + \nabla(\rho u) = \frac{\dot{S}_M}{V} \tag{2.1}$$

The time dependent source term $\dot{S}_M$ represents mass transfer due to evaporation from liquid phase. The momentum conservation is given by Eq 2.2

$$\frac{\partial \rho u}{\partial t} + \nabla(\rho u u) = -\nabla p + \nabla \sigma + F_j + \frac{\dot{S}_I}{V} - \frac{2}{3}\nabla \rho k \tag{2.2}$$

The time dependent momentum source term $\dot{S}_I$ represents momentum transfer from the liquid phase. F_j stands for external forces (such as buoyancy, gravity). The energy equation is given by Eq 2.3

$$\frac{\partial \rho h}{\partial t} + \nabla(\rho u h) = -\frac{Dp}{Dt} + \nabla(\lambda \nabla T) + \frac{\dot{S_E}}{V} \tag{2.3}$$

Where the time dependent source term $\dot{S_E}$ represents energy transfer from liquid phase.

2.2 VSB2 model

The spray model used in this work is VSB2 spray model. VSB2 stands for stochastic blob and bubble spray model. VSB2 is a discrete multicomponent fuel spray lagrangian model which solves for the position, mass and energy of liquid droplets. It treats spray and breakup as one process thereby reducing the required tuning parameters for each spray submodel. The blob and bubble concepts are explained in the following sections.

2.2.1 The blob approach

The main difference between VSB2 and standard models, is that while standard spray models use parcels to solve lagrangian equations, the VSB2 model uses blobs. Parcels consist of equally sized droplets, where the contribution of one droplet is summed up over all the droplets to obtain parcel contribution. Blobs on the other hand contain unequally sized droplets where the size of droplets is based on a distribution function.

The size of droplets is determined by local conditions around the droplet and therefore the distribution of droplets in a blob is more realistic than equally sized droplets as assumed by parcel approach. The contribution of each size interval is summed up to obtain the blob contribution. In the parcel approach a size distribution is considered as well, but it is predescribed and given as the initial condition. While this approach would improve vapor distribution in the vicinity of nozzle, it creates a problem where large droplets will vaporize slowly and smaller droplets vaporize quickly, leading in unrealistic downstream vapor distribution. The use of initial size distribution can be applied to VSB2 model as well however, it does not give the problem mentioned above due to different treatment of droplets in blobs vs parcels.

2.2.2 The bubble approach

In order to minimise grid dependency, the blob interacts with surrounding volume enclosed by a bubble. The volume of bubble is less than or equal to grid cell. For larger grid cells, the volume of bubble is much smaller than grid cell. A schematic of blob and bubble concept is shown in Figure 2.1

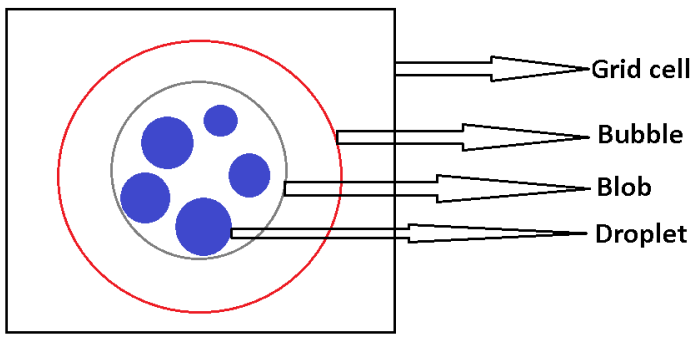

Figure 2.1: *Blob and bubble concept*

The bubble size controls rate of evaporation in large grid cells. The diameter of bubble is given by Eq 2.4

$$D_{bub} = D_B + l_t \tag{2.4}$$

where D_B is blob diameter and the turbulent length scale l_t is given by Eq 2.5

$$l_t = C_\mu^{\frac{3}{4}} \frac{k^{\frac{3}{2}}}{\epsilon} \tag{2.5}$$

The volume of bubble is given by 2.6.

$$V_{bub} = N_D \frac{\pi}{6}[(D_B + l_t)^3 - D_B^3] \tag{2.6}$$

2.2.3 Secondary breakup

The size of droplet as a result of secondary breakup is given by 2.7

$$D' = D_s + (D_{max} - D_s)e^{\frac{-\Delta t}{\tau_{breakup}}} \tag{2.7}$$

where D' is the new droplet diameter after breakup, D_{max} is the initial droplet diameter and D_s is the stable droplet diameter. Δt is computational time step and $\tau_{breakup}$ is breakup time constant and it is obtained from the correlations of Pilch and Erdman. D_s is given by Eq 2.8

$$D_s = We_{cr}\sigma/(\rho_{gas}U_{rel}^2) \tag{2.8}$$

critical weber number is given as

$$We_{cr} = 12(1 + 1.077Oh^{1.6}) \tag{2.9}$$

Oh represents Ohnesorge number and its a function of reynolds and weber number. The size distribution of droplets in a blob is given by a one parameter pdf. The parameter is called power coefficient f. Pdf takes the form given by 2.10

$$D = M^f \tag{2.10}$$

where D corresponds to normalized droplet size and M corresponds to normalized droplet mass. The droplet size is normalized by D_{max} and droplet mass is normalised by the mass corresponding to a droplet of size D_{max}. The normalised droplet mass is divided into 10 mass packages. The first mass package (or first size interval) is given by stripped off mass, which is the mass removed between previous and current timestep due to breakup. The remaining mass is divided into 9 equal packages (intervals). The size of each interval is calculated from the corresponding mass using Eq 2.10.

2.2.4 Relaxation equations

The mass, energy and momentum transfer are solved for each of these mass packages, and then summed up to get blob contribution. The mass transfer is given by relaxation equation (Eq 2.11). Relaxation equation means that the physical quantity that is under consideration is relaxed for every computational timestep. It is a differential equation calculating rate of change of a physical quantity. Using relaxation equation ensures that there is no overshoot or undershoot in the physical quantities.

$$\frac{dm_{evap,ij}}{dt} = -\frac{m_{evap,j} - m_{sc,j}}{\tau_{m,ij}} \tag{2.11}$$

where i denotes a specific mass package and j denotes a specific fuel component. $m_{evap,ij}$ is the evaporated mass for mass package i and fuel component j; $m_{sc,j}$ is the mass

evaporated supercritically for fuel component j. $\tau_{m,ij}$ is the evaporation time constant for mass package i and fuel component j. The supercritically evaporated mass is independent of time as it's assumed to be an instantaneous process. The mass that is left behind after evaporation is referred to as equilibrium mass.

$$m_{eq} = m_{blob} - m_{evap} \tag{2.12}$$

where m_{evap} is the total evaporated mass (summed up over all mass packages). The heat transfer is given by 2.13

$$\frac{dT_{blob,ij}}{dt} = \frac{T_{eq} - T_{blob,ij}}{\tau_{T,ij}} \tag{2.13}$$

where T_{eq} is equilibrium temperature which is temperature of blob after evaporation. It is calculated from energy balance after mass transfer has occured. $T_{blob,ij}$ is the temperature of mass package i and fuel component j and $\tau_{T,ij}$ is evaporation time constant. Details of how $\tau_{T,ij}$ and $\tau_{m,ij}$ and T_{eq} are calculated, can be found in [8]. m_{eq} is calculated using direct numerical method which is explained in next section.

The momentum transfer is also calculated using relaxation equation. $\tau_{U,ij}$ is momentum time constant for mass package package i and fuel component j. U_{eq} is the equilibrium velocity. The blob velocity is obtained using Eq 2.14

$$\frac{dU_{blob,ij}}{dt} = \frac{U_{eq} - U_{blob,ij}}{\tau_{U,ij}} \tag{2.14}$$

2.3 Calculation of equilibrium mass - A direct numerical method

A conceptual picture of evaporation of blob is shown in Figure 2.2.
Heat is transferred from bubble (surrounding air) to the blob (liquid droplets) causing the droplets to evaporate. Evaporation of each fuel component takes place until its saturated mass fraction is reached. The saturated fuel mass fraction is given by Eq 2.15

$$y_{fu,sat,i} = \frac{M_{fu,i}}{M_{mix}} \frac{P_{sat,i}(T_{bub})}{P} X_{liq,i} \tag{2.15}$$

where $y_{fu,sat,i}$ is saturated mass fraction for fuel component i, $M_{fu,i}$ is the molecular weight of fuel component i, $M_{mix,i}$ is the molecular weight of mixture in the gas phase, $P_{sat,i}$ is saturated vapor pressure of fuel component i, P is the gas pressure, and $X_{liq,i}$ is mole fraction of fuel component i in liquid droplet. The above equation is referred to as ideal Roults law, ideal because molecular ineractions are not taken into account. Non-ideal Roult's law is discussed in a later section.

Consequently due to evporation, mass and ethalpy are transferred to the bubble leading to a change in the bubble's mass fraction and enthalpy. The change in mass fraction and enthalpy of bubble inturn result in change of bubble temperature. Thus, evaporation

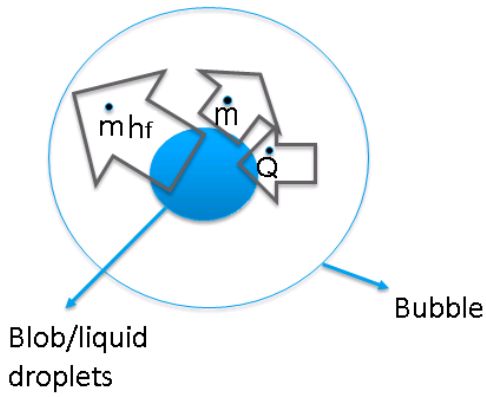

Figure 2.2: *Evaporation of blob in a bubble*

alters the mass fraction of all species, gas enthalpy and gas temperature respectively. These processes are represented by Eq 2.16- Eq 2.19

$$\Delta m_i = f(y_{fu,eq,i}) \tag{2.16}$$

$$y_i' = \frac{y_i m + \Delta m_i}{m + \sum_1^{N_f} \Delta m_i} \tag{2.17}$$

$$h_g' = \frac{m h_g + \sum_1^{N_f} \Delta m_i [h_{liq,i}(Tdr) - \Delta h_{vap,i}(T_{dr})]}{m + \sum_1^{N_f} \Delta m_i} \tag{2.18}$$

$$T' = Temperature(h_g', T_{guess}, y') \tag{2.19}$$

where Δm_i is mass of fuel component i that has evaporated until saturation; y_i', h_g', and T' are the iterative mass fraction, enthalpy and temperature respectively for the gas phase. The set of non-linear equations shown above, are solved simultaneously using SUNDIALS' KINSOL solver. SUNDIALS is a software package that provides time integrators and non-linear solvers which can be coupled with CFD codes. KINSOL is the specific solver package of SUNDIALS that is used to solve non-linear alebraic equation systems. This method of solution is referred to as direct numerical method and it is summerized schematically in Figure 2.3.

The solution to the equations give equilibrium mass that is then used in Eq 2.12. In previous implementation the equations represented by Figure 2.3 were solved iteratively. The problem with iterative method is that it becomes complicated when the number of fuel components increase, making the implementation very difficult.

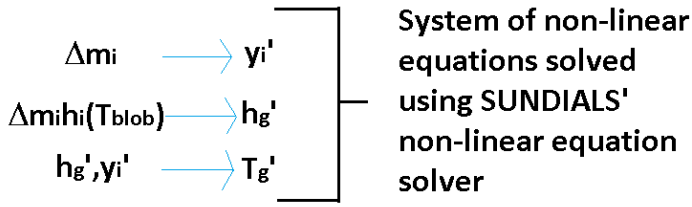

Figure 2.3: *Direct numerical method*

2.4 Vapor-liquid equilibrium (Influence of considering non-ideal thermodynamics)

Vapor liquid equilibrium (VLE) is the steady state condition that is reached when the saturation vapor pressure of liquid and vapor pressure of fuel are equal. Evaporation stops when this condition is reached. In most of the works vapor liquid equilibrium is given by Raoult's law assuming ideal thermodynamics (Eq 2.15). Ideal thermodynamics neglects inter-molecular interactions to simplify VLE. The ideal assumption works well for single component fuels, however in the case of multicomponent fuels especially when polar molecules (alcohols like ethanol) are blended with straight chain alkanes, there is a strong deviation from ideal thermodynamics and this anomaly has been observed to increase with increase in alcohol content.

Non-ideal VLE is achieved when the fuagacities of vapor and liquid phase are equal. The liquid fugacity is a function of (among other parameters) activity coefficient γ. γ takes into account the intermolecular forces between different kinds of molecules in a fuel blend and it is calculated using Non-random two liquid (NRTL) method (Eq 2.20).

$$ln\gamma_i = \frac{\sum_{j=1}^{K} X_{j,l} G_{ji}(T)\tau_{ji}(T)}{\sum_{k=1}^{K} X_{k,l} G_{ki}(T)} + \sum_{j=1}^{K} \frac{X_{j,l} G_{ji}(T)}{\sum_{k=1}^{K} X_{k,l} G_{kj}(T)} (\tau_{i,j}(T) - \frac{\sum_{n=1}^{K} X_{n,l} G_{ni}(T)\tau_{ni}(T)}{\sum_{n=1}^{K} X_{k,l} G_{kj}(T)}) \tag{2.20}$$

where the binary coefficients $G_{i,j}$ and $\tau_{i,j}$ are given by

$$G_{i,j} = e^{-\alpha_{i,j}\tau_{i,j}} \tag{2.21}$$

$$\tau_{i,j} = A_{i,j} + \frac{B_{i,j}}{T} \tag{2.22}$$

$$\alpha_{i,j} = C_{i,j} + D_{i,j} \tag{2.23}$$

The coefficients $A_{i,j} - D_{i,j}$ are obtained from database of chemical engineering software, Aspen plus. They are based on experimental data, but however they can also be determined by UNIQUAC Functional-group Activity Coefficients (UNIFAC) method [9].

In NRTL method, excess thermodynamic functions (such as Gibbs free energy) are used to express deviation from ideal VLE. For futher details the reader can refer to [10]. The NRTL method is used in this work because it has been tested for a wide range of mixtures and also utilizes mininmal assumptions and adjusting parameters compared to other non-ideal VLE models.
Taking activitiy coefficient γ into consideration, the modified Raoult's law for non-ideal thermodynamic equilibrium is obtained (Eq 2.24)

$$y_{fu,eq,i} = \frac{M_{fu,i}}{M_{mix}} \frac{P_{sat,i}(T_{bub})}{P} X_{i,l} \gamma_i \theta_i \tag{2.24}$$

θ_i in 2.24 is gas phase correction factor. For moderate pressures (relevant to operating pressure conditions used in this work) θ_i can be assumed to be unity [11]. $y_{fu,eq,i}$ from equation 2.24 is used to calculate equilibrium mass ($m_{eq,i}$) to be used in VSB2 models' direct numerical method 2.16. This is how non-ideal VLE interfaces with VSB2.

2.5 VLE for ethanol/iso-octane blend

As a first illustration of the influence of non-ideal thermodynamics, VLE for ethanol/iso-octane blend at atmospheric pressure is calculated from Eq 2.25

$$P = \sum P_{vap,i}(T) X_{i,l} \gamma_i \tag{2.25}$$

where P is mixture pressure and $P_{vap,i}$ is the saturated vapor pressure of each component. The mixture pressure is fixed at 1.013 bar. Varying temperature, equilibrium is found using Eq 2.25 and plotted in Figure 2.4.

The plot is boiling temperature of mixture versus mole fraction of iso-octane. It is seen that while for the ideal case there is a continuous increase of temperature, for non-ideal case there is a different trend. For lower iso-octane content (higher ethanol content), the boiling point of mixture decreases, whereas for higher iso-octane content, the boiling point increases following the trend of ideal VLE. A similar trend was observed in an experimental work on vapor-liquid equilibrium of ethanol/iso-octane binary mixture [12], where for lower iso-octane content there was a strong deviation from ideal behavior. It is therefore inferred that modified Raoult's law should be taken into consideration when studying evaporation of multicomponent mixture and this was the motivation to include non-ideal VLE in VSB2 spray model to study evaporation of multicomponent fuel blends.

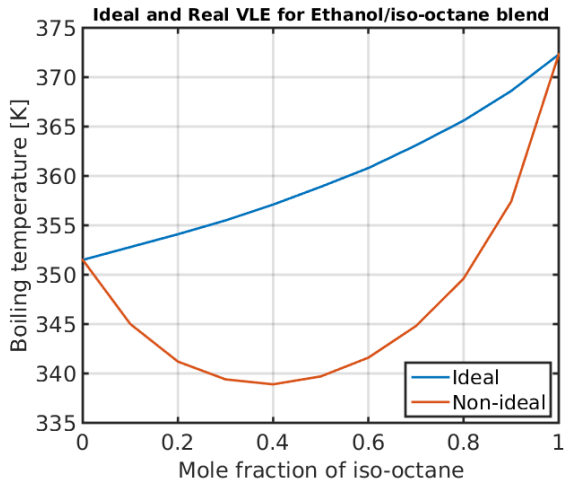

Figure 2.4: *VLE of ethanol/iso-octane mixture at 1.013 bar ambient pressure*

It should be noted that the point of minima for boiling temperature curve in non-ideal case is the azeotropic mixture concentration for ethanol/iso-octane blend (40% volume of iso-octane). At this mixture composition, it is not possible to separate the two components by distillation. As mentioned earler, to the left of azeotrope point where there is higher ethanol content, there is a strong deviation from ideal behavior. This observation will be referred to again in chapter 4 when discussing some results from 3D simulations.

2.6 Turbulence modelling

The turbulence model used for the gas phase in this work is the standard two equation $k-\epsilon$ model. It is used to model the unclosed terms arising from Reynolds Averaged Navier Stokes equation (RANS). This model was originally developed for incompressible flows [13] and was later modified to describe compressible flows [14]. The transport equation for turbulent kinetic energy k, is given by Eq 2.26

$$\frac{\partial \rho k}{\partial t} + \nabla(\rho k u) = \nabla[(\frac{\mu_t}{\sigma_k} + \mu)\nabla k] + \mu_t[S - \frac{2}{3}(\nabla u)^2] - \frac{2}{3}\rho k \nabla u - \rho\epsilon \tag{2.26}$$

The transport transport equation for dissipation of turbulent energy ϵ is by Eq 2.27

$$\frac{\partial \rho \epsilon}{\partial t} + \nabla(\rho \epsilon u) = \nabla[(\frac{\mu_t}{\sigma_\epsilon} + \mu)\nabla \epsilon] + \mu_t C1 \frac{\epsilon}{k}[S - \frac{2}{3}(\nabla u)^2] - \frac{2}{3}C1\rho\epsilon\nabla u - C2\rho\frac{\epsilon^2}{k} + C3\rho\epsilon\nabla u \tag{2.27}$$

where S is given by Eq 2.28

$$S = 2S_{ij}S_{ij} = \frac{1}{2}(\frac{\partial u_j}{\partial x_i} + \frac{\partial u_i}{\partial x_j})^2 \tag{2.28}$$

The coefficients C1-C3 of $k-\epsilon$ model are given as inputs. σ_ϵ is given by Rodi's correlation [15] (Eq 2.29)

$$\sigma_\epsilon = \frac{\kappa^2}{C_\mu^2(C_2 - C_1)} \tag{2.29}$$

3 Case setup

This chapter describes the computational setup and a provides an overview of the experimental setup from whose measurements the model predictions are compared to.

3.1 Experimental setup

The focus of this work is on computational simulations. However a brief description of the experimental setup is given here so as to highlight the quantities being compared in simulations and also the boundary conditions and assumptions. The experimental setup consists of a constant volume combustion vessel that depicts the combustion phase of internal combustion engine's operation. The temperature and pressure in the combustion vessel is therefore those that prevail at end of compression stroke. The focus of these experiments and simulations are therefore on spray formation and combustion alone to get a deeper insight in fuel sprays, rather than the entire engine cycle.

The combustion vessel has the dimension of a cube. Optical access is provided to the combustion vessel through transparent windows on the surfaces of the cube. For schematics of the combustion vessel, the reader can refer to the experimental setup at ECN for example [16]. In the experiments used for comparision in this work, liquid spray penetration is measured by shadowgraphy and vapor penetration by Schliren imaging technique. The internal gas flow is around 10 cm/s and can be assumed to be negligible (in the simulations) compared to the injection velocity of around 600 m/s.

3.2 Computational setup

3.2.1 Computaional mesh

All the simulations are performed using CFD code OpenFOAM version 2.2. Simulations are performed using 3D grid for a constant volume combustion chamber geometry similar to the one used in experiments. The 3D grid shape is that of a cylinder. Top view of the cylinder is shown in Figure 3.1a. The injector is placed in middle of the xy plane (the plane shown in Figure 3.1a), and injection is in the negative z-direction. The full cylinder mesh is shown in 3.1b. The mesh is refined in the centre region around the spray, and coarse outside in order to provide a higher grid resolution to the spray region.

3.2.2 Submodels used

The submodels used for simulations are summarised in Table 3.1. Breakup, mass transfer, heat transfer and drag submodels use relaxation equations. Relaxation equations were described earlier under the subsection 2.2.4 in chapter 2. In short it is a differential equation calculating rate of change of a physical quantity. The physical quantity is droplet radius in breakup model, evaporated mass in mass transfer, blob temperature in heat

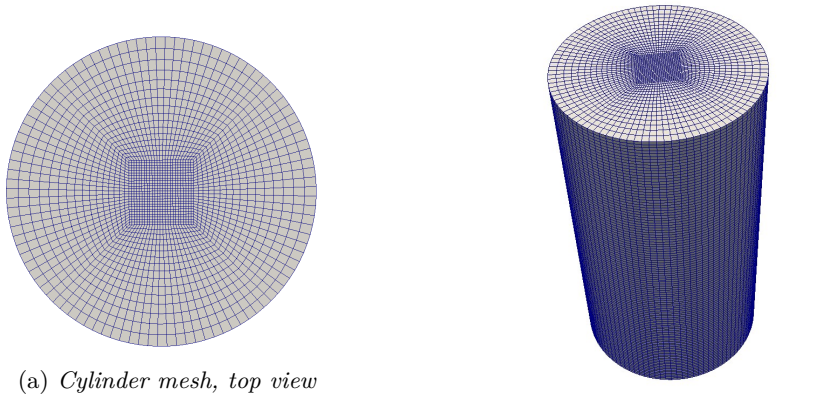

(a) *Cylinder mesh, top view*

(b) *Cylinder mesh, 3D view*

Figure 3.1: *Computational mesh*

transfer and blob velocity in case of drag model. The time constant in breakup model is calculated using the correlations of Pilch and Erdman [17].

The injector model determines the type of spray under study. The injector model used is solid cone injector model. Solid cone sprays have an entire circular impact area at the base of conical spray. The VSB2 model does not use collision models as collision has been known to be very less frequent for solid cone sprays. Atomization model is not used as blob injection method is followed where the diameter of injected blob is equal to nozzle diameter. The injector used is unit injector. The main difference between the different injectors is the way in which velocity is calculated. In unit injector velocity is calculated from input mass flow rate profile as shown in Eq 3.1

$$U = \frac{\dot{m}}{\rho C_D A} \tag{3.1}$$

The droplets (contained in parcels) are injected in a disc with center as injector position and diameter as nozzle diameter. Dispersion model is used to calculate the turbulent velocity of droplets by using turbulent dispersion model. The stochasticDispersionRAS model is used in this work, where the turbulent velocity is sampled from a guassian distribution with variance calculated from k and ϵ that is obtained from turbulence model. The turbulence model used is $k - \epsilon$ model with the coefficients fine tuned for the case under study.

Table 3.1: Submodels used

Submodel	Name
Breakup	Pilch Erdman/Relaxation equation
Mass Transfer	Relaxation equation
Heat Transfer	Relaxation equation
Drag	Relaxation equation
Collision	None
Atomization	None
Injector model (type of spray)	Solid cone
Injector (Injector setup)	Unit injector
Dispersion model	stochasticDispersionRAS

To reduce grid dependency, the turbulent length scale (l_t) is fixed in the code in the injection cell. This is done to ensure $l_t = L_{sgs}$, where L_{sgs} is set to nozzle diameter. If l_t has to be equal to L_{sgs}, ϵ has to satisfy Eq 3.2

$$\epsilon = C_\mu \frac{k^{\frac{3}{2}}}{L_{sgs}} \tag{3.2}$$

4 Summary of results

This chapter summarises two recent publications in Society of Automotive Engineers (SAE) International.

4.1 Summary of publication A - Development and validation of a multicomponent fuel spray model (VSB2 model)

This publication presents the results of extending VSB2 model with a direct numerical method to handle multicomponent evaporating fuel spray. A direct numerical method for solving evaporation and obtaining equilibrium mass was devloped. The direct numerical method was developed to replace previously used iterative method to calculate evaporation. This is because while iterative method was straightforward to implement for single component fuels, it was complicated to implement differential evaporation for multicomponent fuels. The complexity increased with the number of fuel components. The multicomponent fuel model with direct numerical method, is implemented in OpenFOAM-2.2.x to study two-component evaporating fuel spray comprising of n-dodecane and iso-octane in a constant volume combustion vessel. Parts of simulation predictions are compared to experimental data published by Zheng [18]. The quantities measured in simulations are liquid and vapor penetration, evaporation rate, vapor mass fraction, and gas temperature influence on differential evaporation. Four compositions of ethanol and iso-octane were measured-G0, G20, G40, G60. Each of these composition was denoted by Gxx where xx is the percentage by volume of iso-octane in the blend. Boundary conditions are summarised in Table 4.1

Table 4.1: Boundary conditions for publication A

Ambient Temperature	830 K
Ambient Pressure	40 bar
Injection Pressure	800 bar
Injection duration	5.6 ms
Nozzle orifice diameter	160 μm
Injected mass	24.65 mg

The liquid penetration was measured and plotted against experiments and shown in Figure 4.1a. The qualitiative trend resembled that of experimental data. Increasing iso-octane content decreased the liquid penetration as expected since iso-octane is lighter and evaporates faster than n-dodecane. Quantitatively G0 liquid penetration from simulation slightly underpredicts the experiment, whereas for the other cases, there is a good agreement with the experiment. The vapor penetration trend is shown in Figure 4.1b.

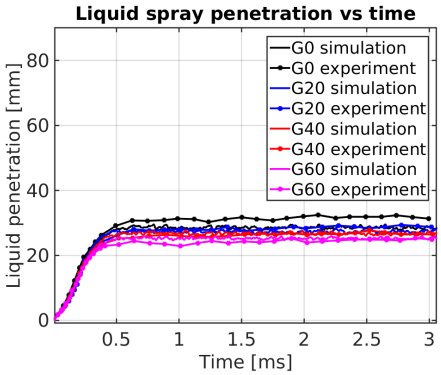

(a) *Liquid penetration versus time*

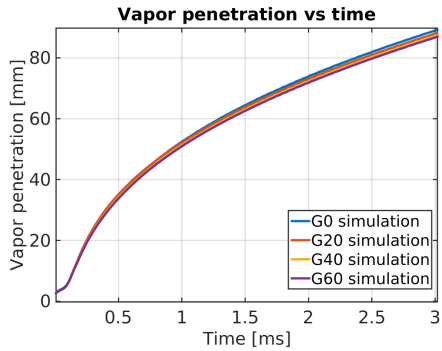

(b) *Vapor penetration versus time*

Figure 4.1: *Liquid and vapor penetration results for Gasoline/Diesel blend*

It follows a similar trend as that of liquid penetration but the difference is smaller because momentum transfer from liquid to gas phase is similar for all the cases. The difference arises from liquid penetration. A contour plot of vapor mass fraction for n-dodecane and iso-octane from G20 case (Figure 4.2a, 4.2b) shows the difference in evaporation clearly. Iso-octane is seen to have a peak closer to the injector since it is lighter and evaporates faster. The area of n-dodecane vapor is larger since it has the higher fraction in the blend (80 %).

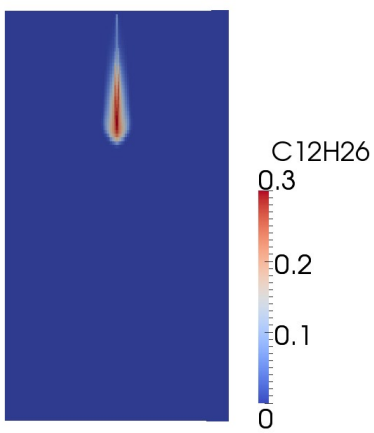

(a) *vapor mass fraction of n-dodecane at 0.5ms*

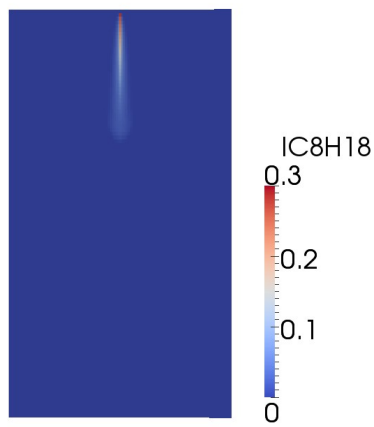

(b) *vapor mass fraction of iso-octane at 0.5ms*

Figure 4.2: *Surface plot of fuel vapor for G20 case*

4.2 Summary of publication B - Influence of considering non-ideal thermodynamics on droplet evaporation and spray formation

This publication presents an argument for the importance of considering non-ideal VLE specifically for alcohols blended with alkanes. Non-ideal VLE is taken into account by including a term called activity coefficient (γ) in combination with ideal Roult's law to calculate vapor liquid equilibrium. Activity coefficient is calulated using Non-random two liquid (NRTL) approach [10]. γ represents the interaction different kinds of molecules and the NRTL approach uses excess thermodynamic functions like excess Gibbs energy, to calculate deviation from ideal behavior. The modified Raoult's law, including activity coefficient is given by Eq 4.1

$$y_{fu,eq,i} = \frac{M_{fu,i}}{M_{mix}} \frac{P_{sat,i}(T_{bub})}{P} X_{i,l} \gamma_i \theta_i \tag{4.1}$$

A 0D plot of boiling temperature of mixture versus mole fraction of iso-octane for ethanol/iso-octane blend at atmospheric pressure is shown in Figure 4.3. It is seen that for

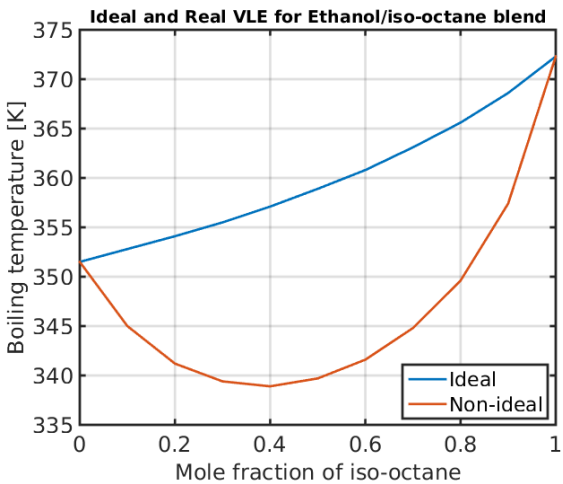

Figure 4.3: *VLE of ethanol/iso-octane mixture at 1.013 bar ambient pressure*

higher ethanol fraction (lower iso-octane), the trend is opposite that of ideal VLE behavior. Similar trend was also observed in an experimental work [12]. The deviation from ideal behavior is due to influence of ethanol on iso-octane molecules. This was a motivation to further analyse ethanol/iso-octane blends using 3D simulations in OpenFOAM-2.2.x. A two-component fuel spray comprising of ethanol and iso-octane is injected into a constant volume combustion vessel with boundary conditions similar to experiments performed by Knorsch et al.[19] (the experimental data was also used in [11]). The blends of ethanol are represented as Exx where xx denotes percentage of ethanol by volume in the blend. The

parameters guaged in this study are liquid and vapor penetration, vapor mass fraction and evaporation rate. Boundary conditions are summarised in Table 4.2

Table 4.2: Boundary conditions for publication B

Ambient Temperature	473 K
Ambient Pressure	5.6 bar
Injection Pressure	200 bar
Injection duration	1 ms
Nozzle orifice diameter	0.2 mm
Injected mass	16 mg

The liquid and vapor penetration comparisons between experiment and simulation for E0 case are shown in Figure 4.4a and 4.4b. The liquid penetration simulations show a

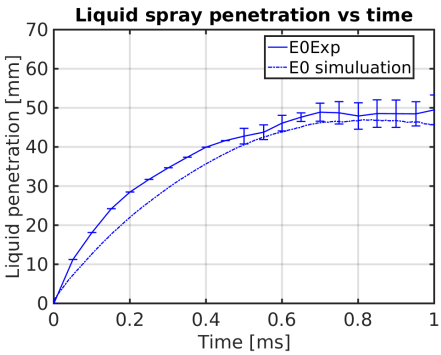

(a) *Liquid spray penetration for iso-octane*

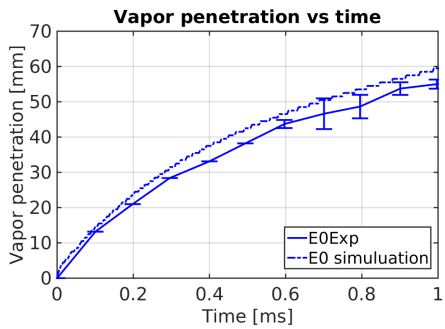

(b) *Vapor penetration for iso-octane*

Figure 4.4: *Liquid and vapor penetration for iso-octane*

reasonable agreement in the later part. The transient part is however not well captured by the simulations and this is probably because the mesh is still coarse to resolve tubulence properties. The grid size along the spray axis is 1mm which is coarse compared to nozzle diameter of 0.2mm. The vapor penetration predictions shows reasonable agreement with experiment.

To analyze the impact of non-ideal VLE, radial fuel distribution for each of the component is plotted first for E10 case and then for E85 case in Figure 4.5a and 4.5b. It is seen that for E10 case, the difference in distribution between ideal and non-ideal case for both fuel components is relatively small. On the other hand the difference is relatively higher for E85 case. The non-ideal VLE predicts higher vapor mass fraction for E85 case because as pointed out earlier (Figure 4.3) the boiling point of mixture is lowered for higher ethanol content in the mixture. It was therefore inferred that assuming ideal VLE

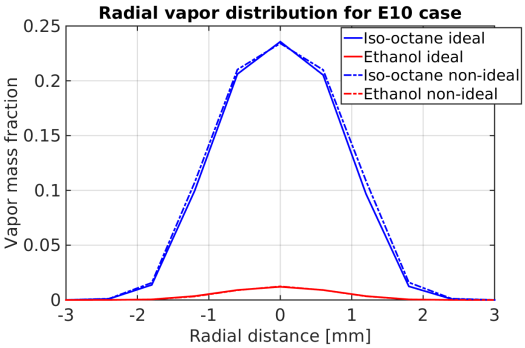

(a) *E10 case*

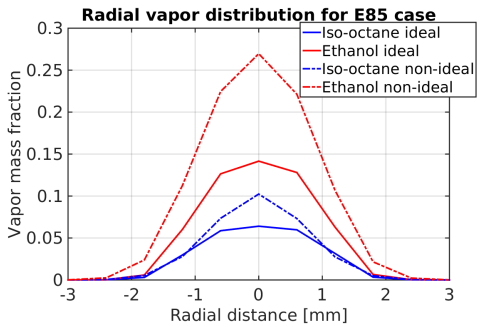

(b) *E85 case*

Figure 4.5: *Radial fuel distribution at t=0.4ms, 35mm from the injector*

in the case of ethanol/iso-octane blend would result in incorrect predictions especially for higher ethanol percentage in the blend. A quantitative statement cannot be made due to the lack of availability of experimental data for E85 case. However similar conclusion has been reported in other works where polar molecules when blended with alkanes tend to form azeotropes which exhibit strong influence on alkanes. Two examples of such works are [19] and [12].

5 Future work

So far VSB2 model has been implemented in open source CFD code OpenFOAM and it has been tested and validated for single and multicomponent fuels. The VSB2 model is also extended to handle non-ideal vapor liquid equilibrium. The future scope of this project are as follows:

5.1 Influence of resolving injector orifice into multiple cells

When computational parcels are injected into one injection cell, then the accuracy of nozzle exit flow profile predictions is believed to be compensated. As a part of future work, the injection orifice will be resolved into multiple cells and the influence of this resolution on spray predictions and nozzle exit flow profile will be studied.

5.2 Multicomponent combusting fuel spray simulations

The impact of differential evaporation in a multicomponent fuel spray on combustion process and emission formation is a consequent topic of interest. It is in the scope of future work to simulate multicomponent combusting fuel sprays and validate the predictions with experimental data.

5.3 Large Eddy Simulation of sprays (LES)

In order to predict air entrainment near the nozzle accurately, and flame lif-off lengths, the accuracy of turbulence models is important. LES method will be used to model the gas phase instead of RANS to get deeper insight into the behavior of sprays and flame fronts. The LES results will be used to identify new terms and/or modify parameters of standard $k - \epsilon$ models that can then be used in industrial applications as LES is computationally expensive.

Nomenclature

Abbreviations

ECN Engine Combustion Network

LES Large Eddy Simulation

NRTL Non-random two liquid

PDF Probability density function

RANS Reynolds Averaged Navier Stokes equation

SAE Society of Automotive Engineers

SUNDIALS Suite of Non linear and Differential/Alebraic Equation Solvers

UNIFAC UNIQUAC Functional-group Activity Coefficients

VLE Vapor Liquid Equilibrium

VSB2 VSB2 Stochastic Blob and Bubble Spray model

List of symbols

ρ	Density of gas
u	Velocity of gas
h	Enthalpy of gas
$\dot{S}_M$	Evaporation source term from spray model
$\dot{S}_I$	Momentum source term from spray model
$\dot{S}_E$	Enthalpy source term from spray model
D_{bub}	Diameter of bubble
D_B	Diameter of blob
$m_{evap,ij}$	Evaporated mass for mass package i and fuel component j
m_{eq}	Mass that is left behind in a blob after evaporation
T_{eq}	Equilibrium temperature of remaining blob after evaporation has occured
U_{eq}	Equilibrium velocity of blob after evaporation has occured
$\tau_{m,ij}$	Evaporation time constant for mass package i and fuel component j
$T_{blob,ij}$	Liquid temperature in the blob for mass package i and fuel component j
$\tau_{T,ij}$	Heat transfer time constant for mass package i and fuel component j
$U_{blob,ij}$	Velocity of blob for mass package i and fuel component j
$\tau_{U,ij}$	Momentum transfer time constant for mass package i and fuel component j
$y_{fu,eq,i}$	Equilibrium fuel mass fraction of fuel component i
$y_{fu,sat,i}$	Same definition as $y_{fu,eq,i}$
T_{bub}	Temperature of bubble
$M_{fu,i}$	Molecular weight of fuel component i
M_{mix}	Molecular weight of gaseous mixture
$P_{sat,i}$	Saturation pressure of fuel component i

$X_{liq,i}$	Mole fraction of fuel component i in liquid droplet
Δm_i	Total evaporated mass for fuel component i until saturation is reached
y_i'	Iterative mass fraction of fuel component i
m	Total mass of the grid cell
N_f	Total number of fuel components
h_g'	Iterative enthalpy of the surrounding gas (in grid cell)
$h_{liq,i}$	Liquid enthalpy of fuel component i
$\Delta_{hvap,i}$	Enthalpy of vaporization of fuel component i
T_{dr}	Fuel droplet temperature
T'	Iterative temperature of the gas
γ_i	Iterative temperature of the gas
θ_i	Iterative temperature of the gas
P	Pressure of gas
$P_{vap,i}$	Vapor pressure of fuel component i
k	Turbulent kinetic energy
ϵ	Turbulent dissipation
μ_t	Turbulent viscocity
σ	Stress tensor

Bibliography

[1] International energy agency. *World Energy Outlook, 2017*. URL: https://www.iea.org/weo2017/.

[2] European Commission. *2020 renewable energy targets*. URL: https://ec.europa.eu/energy/en/topics/renewable-energy.

[3] C.Baumgarten. *Mixture formation in internal combustion engines*. Berlin, Germany: Springer, 2006.

[4] Youngchul Ra and Rolf D. Reitz. "A vaporization model for discrete multi-component fuel sprays". In: *International Journal of Multiphase Flow* 35.2 (2009), pp. 101–117. ISSN: 03019322. DOI: 10.1016/j.ijmultiphaseflow.2008.10.006. URL: http://dx.doi.org/10.1016/j.ijmultiphaseflow.2008.10.006.

[5] Shiyou Yang et al. "Development of a Realistic Multicomponent Fuel Evaporation Model". In: *Atomization and Sprays* 20.11 (2010), pp. 965–981. ISSN: 1044-5110. DOI: 10.1615/AtomizSpr.v20.i11.40.

[6] Engine combustion network. *ECN 1 workshop, Computational Effort Presentations, subtopic: spray A*. 2011. URL: https://ecn.sandia.gov/ecn-workshop/ecn1-proceedings/.

[7] John Abraham. "What is Adequate Resolution in the Numerical Computations of Transient Jets?" In: 412 (1997). DOI: 10.4271/970051. URL: http://papers.sae.org/970051/.

[8] Anne Kosters and Anders Karlsson. "Validation of the VSB2 spray model against spray A and spray H". In: *Atomization and Sprays* 26.8 (2016).

[9] A. Fredenslund, L.R. Jones, and M. Prausnitz. "Group-contribution estimation of activity coefficients in nonideal liquid mixtures". In: *AIChe Jourbal* 21.6 (1975), pp. 1086–1099.

[10] Henri Renon and J M Prausnitz. "Local Compositions in Thermodynamic Excess Functions for Liquid Mixtures". In: *AIChE* 14.1 (), pp. 135–144.

[11] P. Keller et al. "Experimental and numerical analysis of iso-octane/ethanol sprays under gasoline engine conditions". In: *International Journal of Heat and Mass Transfer* 84 (2015), pp. 497–510. ISSN: 00179310. DOI: 10.1016/j.ijheatmasstransfer.2015.01.011. URL: http://dx.doi.org/10.1016/j.ijheatmasstransfer.2015.01.011.

[12] Chao-Cheng Wen and Chein-Hsiun Tu. "Vapor–liquid equilibria for binary and ternary mixtures of ethanol, 2-butanone, and 2,2,4-trimethylpentane at 101.3kPa". In: *Fluid Phase Equilibria* 258.2 (2007), pp. 131–139. ISSN: 03783812. DOI: 10.1016/j.fluid.2007.06.005. URL: http://linkinghub.elsevier.com/retrieve/pii/S0378381207003032.

[13] B E Launder. "H, 0'3". In: 15 (1972), pp. 301–314.

[14] A.D. Goasman and A.P.Watkins. *A computer prediction method for turbulent flow and heat transfer in piston/cylinder assemblies*. 1977.

[15] W. Rodi. “Turbulence model and their application in hydraulics-A state of the art review”. In: *IAHR, Netherlands* 15 (1984).

[16] Engine combustion network. *Combustion Vessel Geometry: 1997 to Present*. URL: https://ecn.sandia.gov/diesel-spray-combustion/sandia-cv/combustion-vessel-geometry/.

[17] M. Pilch and C.a. Erdman. “Use of breakup time data and velocity history data to predict the maximum size of stable fragments for acceleration-induced breakup of a liquid drop”. In: *International Journal of Multiphase Flow* 13.6 (1987), pp. 741–757. ISSN: 03019322. DOI: 10.1016/0301-9322(87)90063-2.

[18] Liang Zheng et al. “An optical study on liquid-phase penetration, flame lift-off location and soot volume fraction distribution of gasoline-diesel blends in a constant volume vessel”. In: *Fuel* 139 (2015), pp. 365–373. ISSN: 00162361. DOI: 10.1016/j.fuel.2014.09.009. URL: http://dx.doi.org/10.1016/j.fuel.2014.09.009.

[19] Tobias Knorsch et al. “On the role of physiochemical properties on evaporation behavior of DISI biofuel sprays”. In: *Experiments in Fluids* 54.6 (2013). ISSN: 07234864. DOI: 10.1007/s00348-013-1522-6.

List of Figures

List of Tables